Digest Journal of Nanomaterials and Biostructures

Dig. J. Nanomater. Bios. **2026**; 21(2): 55239
https://doi.org/10.31083/DJNB55239

Original Research

Preparation of DNA Nanotubes Decorated With Gold Nanoparticles Based on DNA Origami

Xiaohong Yang[1,*], Ganghui Wu[1], Mu Qiao[2], Xia Ye[2]

[1]School of Materials Engineering, Jiangsu University of Technology, 213001 Changzhou, Jiangsu, China
[2]School of Mechanical Engineering, Jiangsu University of Technology, 213001 Changzhou, Jiangsu, China
*Correspondence: 13651502861@126.com (Xiaohong Yang)
Academic Editors: Xiangcheng Sun and Carmen-Georgeta Ristoscu
Submitted: 10 December 2025 Revised: 31 March 2026 Accepted: 10 April 2026 Published: 24 June 2026

Abstract

The controlled arrangement of metal nanoparticles is crucial for the development of plasmonic devices. Deoxyribonucleic acid (DNA) origami provides a template for nanoparticle assembly. Herein, the caDNAno software was used to design double-layered DNA nanotubes with capture sites for gold nanoparticles (AuNPs). Functionalized AuNPs were conjugated to the nanotubes via sequence-specific probe hybridization. The resulting hybrid nanostructures were characterized using agarose gel electrophoresis, atomic force microscopy, and transmission electron microscopy. AuNPs were found to be periodically arranged along the DNA nanotubes in a helical configuration. Ultraviolet–visible spectroscopy revealed a red shift of the localized surface plasmon resonance peak, which indicated plasmonic coupling between the helically arranged nanoparticles. Our method holds promise for optical sensing and detection.

Keywords: DNA origami; DNA nanotube; gold nanoparticles; self-assembly

1. Introduction

The ordered arrangement of nanoparticles is a significant challenge in the field of nanotechnology. DNA, a naturally occurring nanoscale material, provides an excellent template for the ordered arrangement of nanoparticles [1,2,3]. Its unique biological properties, such as enzyme cleavage, splicing, and modification, allow it to be modified with functional groups at specific sites. These groups can then be chemically or electrostatically linked to nanoparticles [4]. These DNA-nanoparticle conjugates can be assembled into specific nanostructures by leveraging the principle of base complementary pairing [5,6]. With the development of DNA nanotechnology, many researchers have explored using DNA as a template for assembling nanoparticles [7,8,9]. Mucic et al. [10] successfully connected gold nanoparticles by modifying the sulfhydryl group at the end of DNA in 1998. Despite this early progress, achieving an ordered assembly of nanoparticles remained a challenge.

With the development of DNA self-assembly technology, a hybrid nanoparticle self-assembly technology has gradually emerged, which utilizes the DNA molecular tiles and DNA origami as templates [11,12]. In this approach, different DNA templates are firstly prepared by DNA self-assembly technology, and then the required sites are designed and then connected with nanoparticles. The precise positioning of these nanoparticles can achieve different optical properties [13].

However, the self-assembly of DNA molecular tiles into structures often presents two major challenges: difficulty in controlling the final size and the inability to precisely manage hybridization sites during the creation of heterostructures. In order to overcome these two problems, double-layered DNA nanotubes were designed using the caDNAno software, and sticky ends were introduced at specific positions. A probe hybridization method was employed to prepare hybrid structures of gold nanoparticles and DNA nanotubes. The resulting structures were characterized via agarose gel electrophoresis, atomic force microscopy (AFM), and transmission electron microscopy (TEM), with preliminary predictions of their potential optical properties.

2. Materials and Methods

2.1 Materials

Polyacrylamide gel electrophoresis (iPAGE) and PAGE-purified DNA primer single strand, agarose were purchased from Invitrogen Biotechnology Co., Ltd (Shanghai, China). 10 nm colloidal gold solution, purchased from Tedpella (Redding, CA, USA); Freeze 'N' Squeeze centrifugal columns, purchased from Bio-rad (Hercules, CA, USA); Centrifugal ultrafiltration tubes of 100 kDa were purchased from Merck Millipore (Billerica, MA, USA); TCEP, ethidium bromide (EB) was purchased from Sigma-Aldrich (St. Louis, MO, USA); GE-25 purification columns were purchased from GE Healthcare Life Sciences (Marlborough, MA, USA); mica flakes, bis(oxy)uranium acetate, carbon-sprayed 400-mesh copper mesh from Beijing Zhongjingkeji Technology Co., Ltd (Beijing, China). All solutions were prepared with ultrapure water.

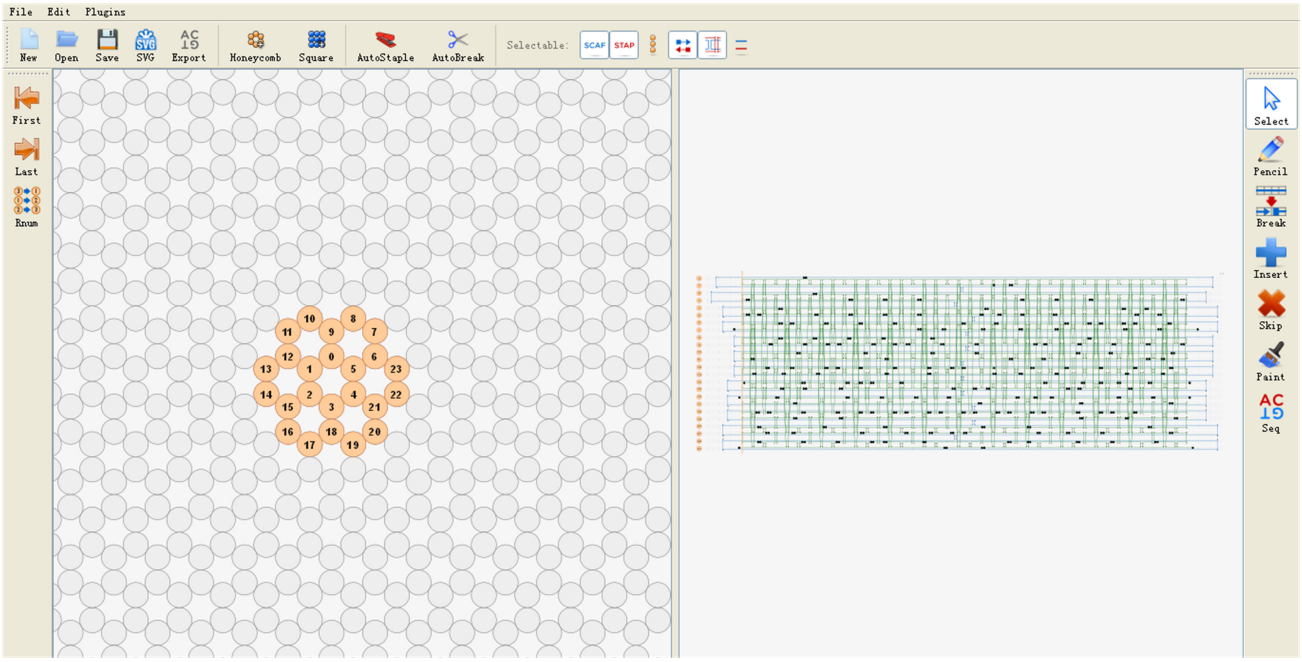

Fig. 1. caDNAno software interface and the designed DNA nanotube origami.

2.2 Design of Origami DNA Nanotubes Hybridized Structures With AuNPs

The DNA nanotube structures were designed using caDNAno [14], a three-dimensional origami software developed by Douglas at the Wyss Institute at Harvard University (v0.2.3, Boston, MA, USA). The software design interface is shown in Fig. 1. The honeycomb region on the left is a cross-sectional view of the DNA nanotube structure we designed, and the region on the right is the origami path of the DNA nanotube, which was made to form the tubular structure we desired through the reasonable use of staple chains to hold the scaffolding chains in place. An image of the detailed design path of the origami DNA nanotubes is shown in Appendix Fig. 8, and the sequence of the stapled strands of the DNA nanotubes is shown in Appendix Table 2.

The double-layer (bilayer) architecture was chosen for its enhanced mechanical rigidity and stability compared to single-layer structures, providing a more robust template for subsequent nanoparticle attachment. The process of assembling DNA nanotubes by DNA origami is as follows: the phage DNA single strand M13mp18 is used as the scaffolding strand, and the corresponding staple strand sequence is obtained through software design and sent to the biological company for synthesis, the staple strands synthesized by the company were mixed with the M13mp18 DNA strand, and the structure required by our design is assembled through base complementary pairing under specific buffer and thermal cycling conditions, whose assembly principle is schematically shown in Fig. 2a. In this paper, DNA nanotubes with a length of around 92 nm and a diameter of around 14 nm were designed.

Some sticky ends (thiolation single-stranded DNA, (SH-ssDNA)) were induced at specific positions of DNA nanotubes, which can hybridize with AuNPs conjugates to form the designed structures. One of the major advantages of building DNA nanostructures by origami is that the modification sites on them are precisely controllable, and the sites of modification can be arbitrarily adjusted according to the needs. In this experiment, 10 different sites on the DNA nanotube are designed, three identical sticky ends protrude from each site, and sticky ends at the neighboring sites are different, which contain a total of two kinds, one at the 5′ end of the DNA strand, and the other at the 3′ end of the DNA strand, all of which are 15 bases in length; the three sticky ends at the 5′ end are connected to an AuNPs, and the three sticky ends at the 3′ end are connected to another AuNPs and so alternately arranged, finally making the AuNPs in a helical shape on the DNA nanotubes. These binding sites are positioned with a specific rotational offset (~120–140°) around the longitudinal axis of the cylindrical nanotube in the 3D design. This spatial arrangement directs the attached AuNPs to occupy positions on different "faces" of the nanotube, thereby promoting a helical configuration around its circumference rather than a linear arrangement. The schematic diagram of the assembly principle of the hybrid structure of DNA nanotubes with AuNPs is shown in Fig. 2b. The picture of the designed pathway of DNA nanotubes containing specific sites is shown in Appendix Fig. 9.

2.3 Origami DNA Nanotube Preparation

The purchased DNA primer single strands (DNA Oligo) were first centrifuged for a few minutes, then dis-

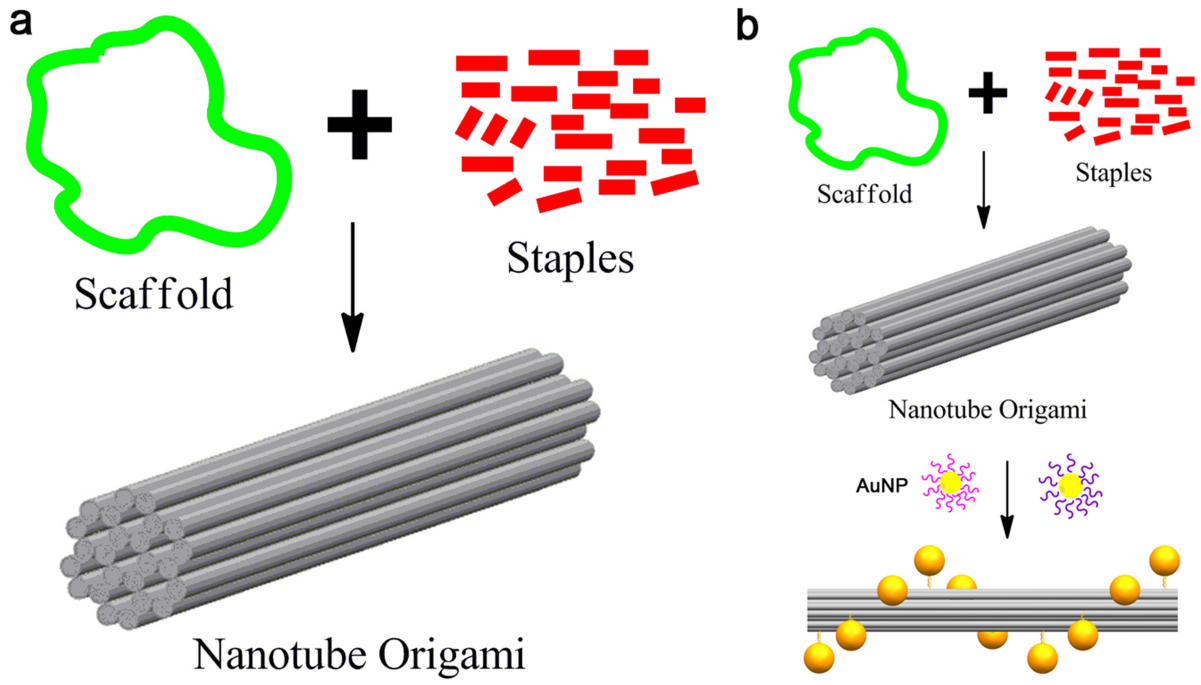

Fig. 2. The schematic diagram of DNA nanotubes and AuNPs. (a) DNA nanotube origami. (b) Its hybrid structure. AuNPs, gold nanoparticles.

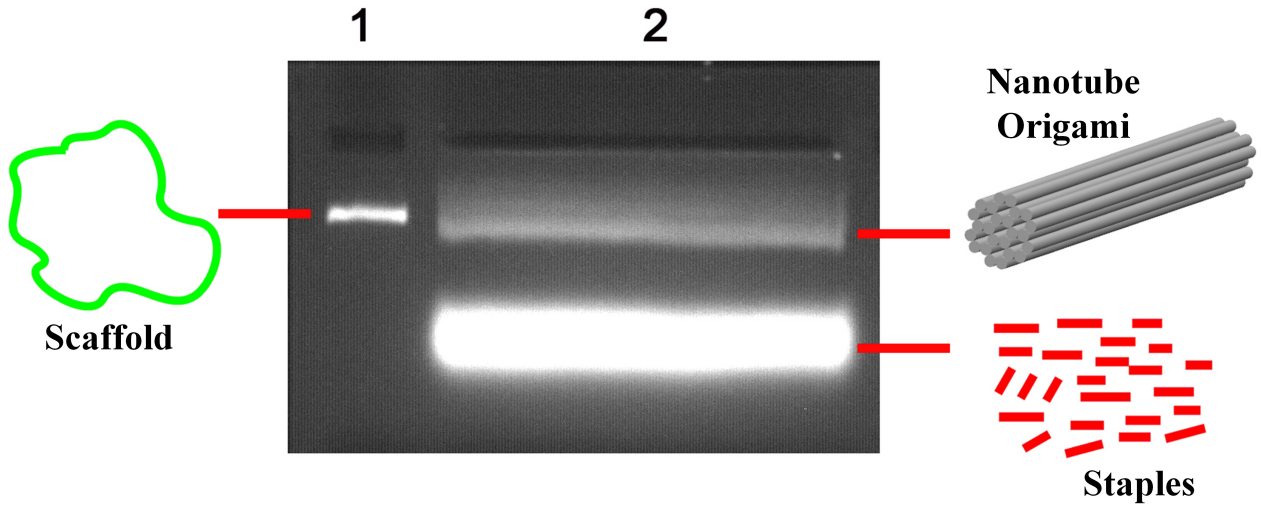

Fig. 3. 1.5% agarose gel electrophoresis image of DNA nanotube origami.

solved in a quantity of ultrapure water, shaken and mixed on a shock mixer, centrifuged again, and formulated into a storage solution at a concentration of 100 µM. 2 µL from each single strand was mixed in a 1.5 mL EP tube, and since the total number of stapled strands was 197, an additional 6 µL of ultrapure water was required to formulate the reaction solution at a concentration of 500 nM. The DNA scaffold strand (M13mp18) and the staple strand were mixed in the buffer at a molar ratio of 1:10, giving a total volume of 100 µL for the final system, with a concentration of c[staples] = 100 nM for the staple strand and c[scaffold] = 10 nM for the scaffold strand. The composition of each substance and the volume required are shown in Table 1. The mixture was placed on a polymerase chain reaction (PCR) instrument (K960, Hangzhou Lattice Scientific Instruments Co., Ltd., Hangzhou, Zhejiang, China) and annealed as follows: 5 min at 80 ℃, then cooled down to 60 ℃ at a cooling rate of 1 ℃/5 min; then cooled down to 24 ℃ at a rate of 0.5 ℃/45 min, with the whole process taking 55 h 40 min.

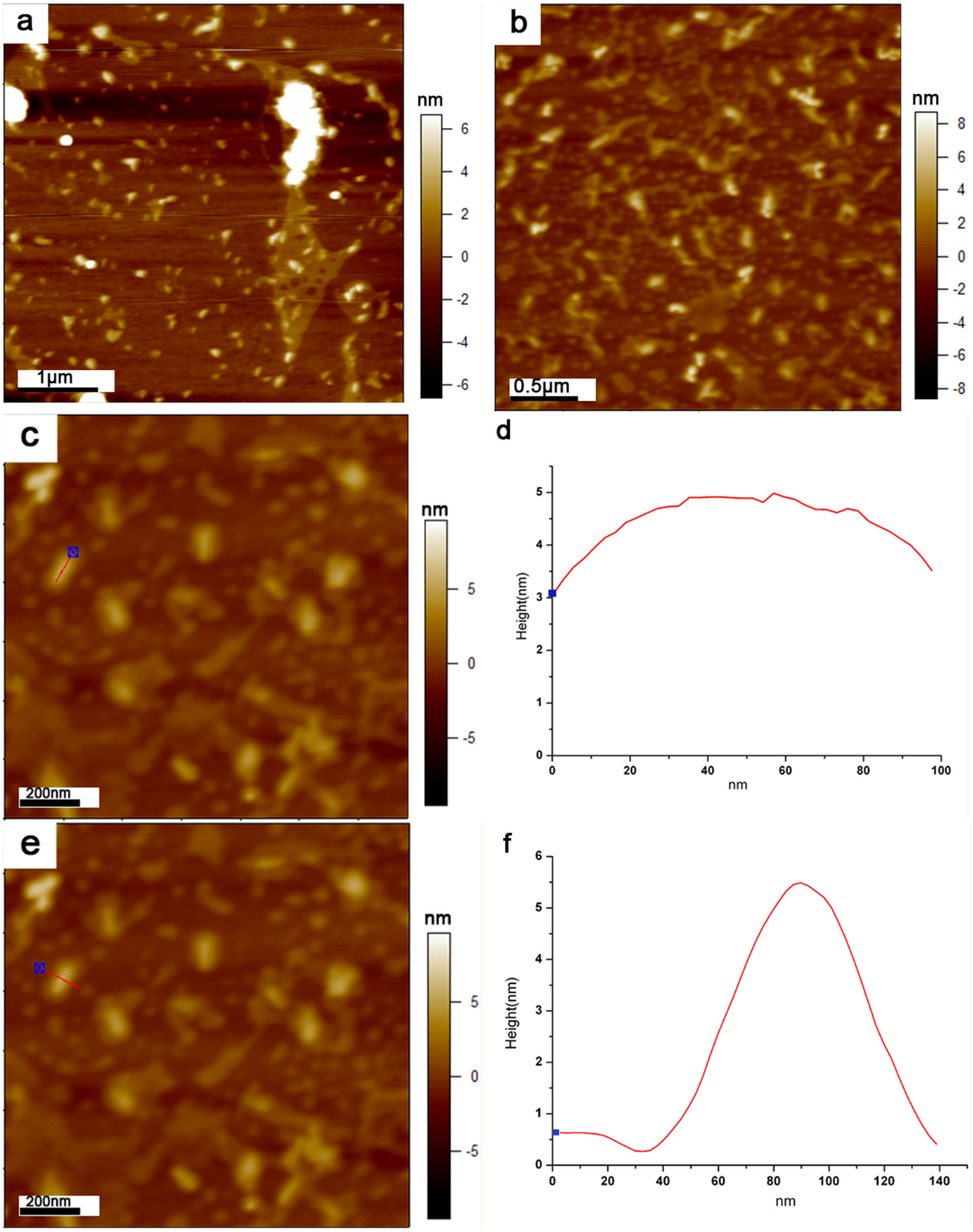

Fig. 4. AFM images and section graph of DNA nanotube origami. (a–c) DNA nanotube. Scale bar = 1 μm in (a); scale bar = 0.5 μm in (b); scale bar = 200 nm in (c,e); (d,f) the height of the nanotube. Vertical height in (d); horizontal height in (f). AFM, atomic force microscopy.

2.4 Hybridization DNA Nanotubes With AuNPs

2.4.1 Reactions of SH-ssDNA-Coated AuNPs

The surface of 10 nm AuNPs was treated with bis(p-sulfophenyl)phenylphosphine dipotassium dihydrate (BSPP) and concentrated; the absorbance of the concentrated gold nanoparticles was measured using an ultraviolet-visible (UV-Vis) spectrophotometer (UV-6100, Shanghai Yuanxi Instruments Co., Ltd., Shanghai, China) and calculated to give a concentration of 1.17 μM. To reduce disulfide bonds in SH-ssDNA to monosulfide bonds, a specific amount of tris(2-carboxyethyl)phosphine (TCEP) was added to the SH-ssDNA single strand. The TCEP concen-

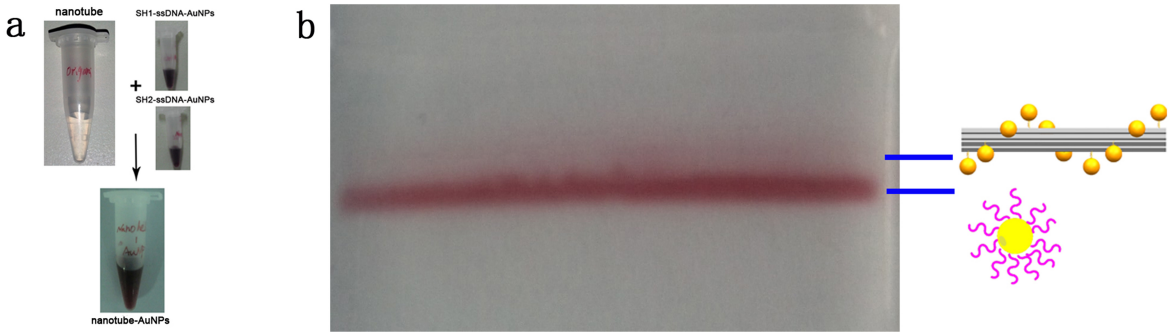

Fig. 5. Hybridization solution and electrophoresis gel. (a) Reaction mixture. (b) Agarose electrophoresis image of hybrid structure.

Table 1. Composition of DNA nanotube origami folding mixture and volume of each component.

Composition	Volume (µL)
Scaffold, 100 nM	10
Staples, 500 nM	20
10× Folding Buffer (50 mM Tris, 10 mM EDTA)	10
ddH_2O	50
140 mM $MgCl_2$ solution	10

EDTA, Ethylenediaminetetraacetic acid.

tration in the mixture was 20 mM, and the mixture was treated at room temperature for 1 hour. Small molecules were removed using a GE-25 purification column. The amount of AuNPs and SH-ssDNA required was calculated according to the molar ratio of 1:300 and mixed in 0.5× TBE (Tris: 89 mM, Boric Acid: 89 mM, EDTA: 2 mM) buffer. An appropriate amount of NaCl was added with a starting concentration of 50 mM, and the reaction was shaken on a shaking table at room temperature. The concentration of NaCl was then increased every 7 h. The concentration of NaCl was increased by 50 mM every time, and the final concentration of NaCl was 300 mM; the whole process was about 40 h. The encapsulated AuNPs were concentrated in a centrifugal ultrafiltration tube at 100 kDa to remove excess mercapto-DNA single strands, and the eluent was 0.5× TBE buffer. This high DNA-to-AuNP ratio was used to ensure high surface coverage for stability, though it may contribute to steric hindrance. The functionalized AuNPs were concentrated in a 100 kDa centrifugal ultrafiltration tube to remove excess thiolated DNA single strands, using 0.5× TBE buffer as the eluent.

2.4.2 Purification of DNA Nanotubes

A 1.5% (m/v) agarose gel was prepared with 10 µL of EB added as a DNA stain. One hundred µL of DNA nanotube samples were mixed with 20 µL of 6× Loading Buffer and added to the lanes of the agarose gel. Electrophoresis was performed for 2 hours in 0.5× TBE buffer (containing 11 mM $MgCl_2$) at 100 V. The desired bands were cut under a UV lamp, mashed into a Freeze 'N' Squeeze centrifuge column, frozen at –20 °C for 10 min, and then centrifuged at 14,000 relative centrifugal force (rcf) for 10 min.

2.4.3 Preparation and Purification of DNA Nanotube-AuNP Hybrid Structures

Mix purified DNA nanotubes with concentrated SH-ssDNA conjugates at a 1:50 ratio. Incubate the mixture on a shaking platform at room temperature for 24 hours. Prepare a 0.5% (w/v) agarose gel. Since gold nanoparticles exhibit a burgundy color, no additional dye is required. Mix the reaction mixture with 50% glycerol in a 5:1 ratio, dispense into agarose gel lanes, and run electrophoresis for 1 hour in 0.5× TBE buffer (containing 11 mM $MgCl_2$) at 120 V. The target bands were cut under white light and mashed into a Freeze 'N'Squeeze centrifuge column, then frozen at –20 °C for 10 min before being centrifuged in a high-speed centrifuge for 10 min (centrifugal force of 14,000 rcf), and remixed well after removing the supernatant with a pipette tip.

3. Results

3.1 Electrophoresis Results of DNA Nanotube

The results of agarose gel electrophoresis for the origami DNA nanotubes are shown in Fig. 3. Lane 1 contains the M13mp18 single-stranded DNA scaffold, while Lane 2 contains the assembled origami DNA nanotube structures. Several distinct bands are visible in Lane 2. The fastest migrating band corresponds to excess staple strands. Due to the significantly higher concentration of staple strands relative to scaffold strands, this band appears brighter under UV illumination. Slightly faster than the M13mp18 scaffold band, a clear band corresponding to the successfully assembled DNA nanotube structures is observed. Additionally, trailing bands appearing above the target band are attributed to nanotube aggregation, resulting in larger, higher-order structures. The electrophoretic mobility of DNA is influenced not only by molecular weight but also by its higher-order conformation. Different DNA conformations possess varying hydrodynamic diameters, resulting in different electrophoretic frictions and thus presenting as multiple bands during electrophoresis. The as-

sembled DNA nanotubes exhibit faster migration than the M13mp18 single strand due to their more compact, linear one-dimensional structure.

3.2 Analysis of AFM of DNA Nanotubes

The AFM (AFM MFP-3D, Asylum Research Company, Santa Barbara, CA, USA) of DNA nanotubes constructed based on DNA origami is shown in Fig. 4. Fig. 4a–c show the AFM of DNA nanotubes in different scanning ranges, and Fig. 4d,f are the height-analysed plots of the same nanotube structure in the transverse and longitudinal directions in Fig. 4c,e, respectively. From the figure, we can observe many fine short rod-like structures; these are the DNA nanotube structures we expected, and since the AFM pictures were obtained before purification of the DNA nanotubes, there are many other DNA impurities on the mica sheet substrate. In order to confirm that these structures match our design, we selected one of the structures and analysed its height in the transverse and longitudinal directions, as shown in Fig. 4d,f, from which it can be seen that the DNA nanotubes have a transverse span of about 25 nm, a longitudinal span of about 90 nm, and a height of more than 5 nm, whereas the DNA nanotubes that we have designed theoretically have a diameter of about 15 nm, the length is around 92 nm, and since the DNA nanotubes will be collapsed under the action of the atomic force needle tip and form a flat structure, they should theoretically be around 24 nm, which matches with the observed results, and it can be determined that these are the Origami DNA nanotubes.

3.3 Analysis of Electrophoretic Results of Hybridized Structures of DNA Nanotubes With AuNPs

Fig. 5a shows physical images of the DNA nanotube reaction system, the SH-ssDNA-AuNPs conjugate reaction system, and the physical picture of the reaction system of the nanotube-AuNPs hybrid structure. The final solution is burgundy in colour, which is the colour of the 10 nm AuNPs. Fig. 5b shows the 0.5% agarose electrophoresis picture of the DNA nanotube-AuNPs heterostructure. From the figure, we see two obvious bands: the dark red band below is the SH-ssDNA-AuNPs conjugate, and the light red band on the top is our target band, i.e., the nanotube-AuNPs heterostructure. The two substances are well separated by electrophoresis due to the large difference in molecular weight. In order to increase the probability of connection, we used an excess of AuNPs in the experiment. Through this step of agarose electrophoresis separation, we can remove the excess AuNPs, so that we can get a relatively pure hybridisation product for the observation of subsequent experiments.

3.4 TEM of the DNA Nanotubes With AuNPs

Fig. 6 shows TEM of DNA nanotube-AuNPs hybrid structures. The magnifications of Fig. 6a–d are different, in which the samples in Fig. 6a–c have been negatively stained by using uranyl acetate, and the sample in Fig. 6d has not been negatively stained. From Fig. 6a,b, we can see that many identical hybridized structures appear in the same field of view and are irregularly arranged on the copper mesh, with some stacked together, which is due to the aggregation and sedimentation during the concentration of the samples. In addition to the characteristic structures, there are numerous discrete gold nanoparticles, which were detached from the hybridized structures during high-speed centrifugation and purification. The samples that have been negatively stained with uranyl acetate, the DNA nanotube structures in the middle are less lined under TEM, but clear short rod-like structures can still be seen, with a length of around 100 nm. From the comparison between the insets in the upper right corner of Fig. 6a,b and the TEM images, we find that the assembled hybridized structure matches well with the expected design, and the AuNPs and the DNA nanotubes are connected through the hydrogen bonding of base pairing, which is still relatively not strong enough and can be easily destroyed under external force, and thus the phenomenon as shown in Fig. 6. Fig. 6c shows the high magnification TEM image after negative staining of the hybridized structure. It can be seen that the AuNPs are helically arranged around the DNA nanotubes. The number of AuNPs is basically in the range of 7–9, and only a very small number of them can reach 10, which is due to the role of repulsive force between the AuNPs, which makes it difficult for the sticky ends at some positions to be connected to the AuNPs, so the connection position of AuNPs needs to be further optimized in the subsequent work. In the sample of Fig. 6d, we cannot see the DNA nanotubes because there is no negative staining, and we only see the AuNPs arranged in a certain regularity in space. This helical structure gives rise to a certain chiral character as calculated by Kuzyk et al. [15], i.e., it has a spinodal character, and due to the low yield of origami, we did not test the relevant properties any further in this paper's study, and will attempt to increase the yield and perform the relevant characterization in subsequent work.

3.5 UV-Vis Spectroscopic Analysis of Origami DNA Nanotube-AuNPs Hybrid Structures

The UV-Vis absorption spectra of the mixture of origami DNA nanotubes and SH-ssDNA-AuNP conjugates before and after the annealing reaction were measured, and the results are shown in Fig. 7. The black curve is the spectrum before annealing, and the red curve is after annealing. A subtle red shift of the characteristic absorption peak from 520 nm to 524 nm is observed. This minor shift could be attributed to a slight change in the local refractive index as AuNPs become associated with the DNA nanotubes, or to very weak plasmonic coupling between a small fraction of nanoparticles in close proximity. The figure shows that the width of the absorption peak of the spectrum of the an-

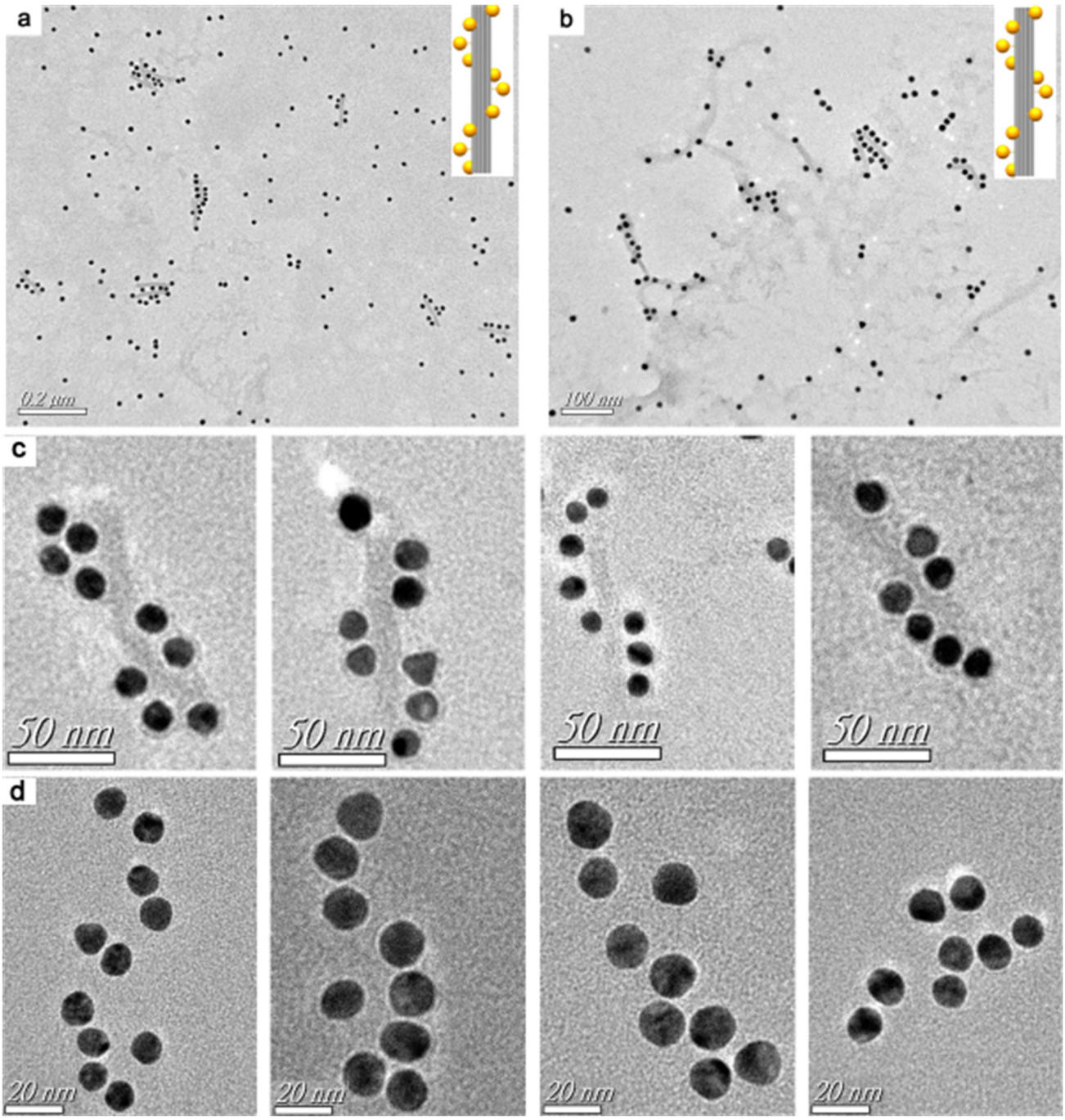

Fig. 6. TEM image of DNA nanotube and AuNPs hybrid structure. (a–c) Hybrid structures at different magnifications (uranyl acetate used for negative staining). (d) Hybrid structure (unstained). Scale bar = 0.2 μm in (a); scale bar = 100 nm in (b); scale bar = 50 nm in (c); scale bar = 20 nm in (d); TEM, transmission electron microscopy.

nealed product is broadened, which is due to the change in the spacing of the Au nanoparticles due to the connection to the origami structure, and the interaction of the free electrons on the surface of the gold nanoparticles, resulting in the broadening of the absorption peak of the AuNPs [16].

4. Discussion

DNA nanotubes with bilayer structure and DNA nanotubes with 30 sticky ends were designed by using the origami design software caDNAno, and the designed DNA nanotube structures were successfully prepared by a one-step reaction method using the M13mp18 strand as the scaffolding strand. The fabricated nanotube structures were characterized by agarose gel electrophoresis and AFM. The results showed that the length of the DNA nanotubes was about 90 nm, and the width of the collapsed nanotubes was about 25 nm with a height of more than 5 nm, which was in accordance with the expected design. The DNA nanotubes

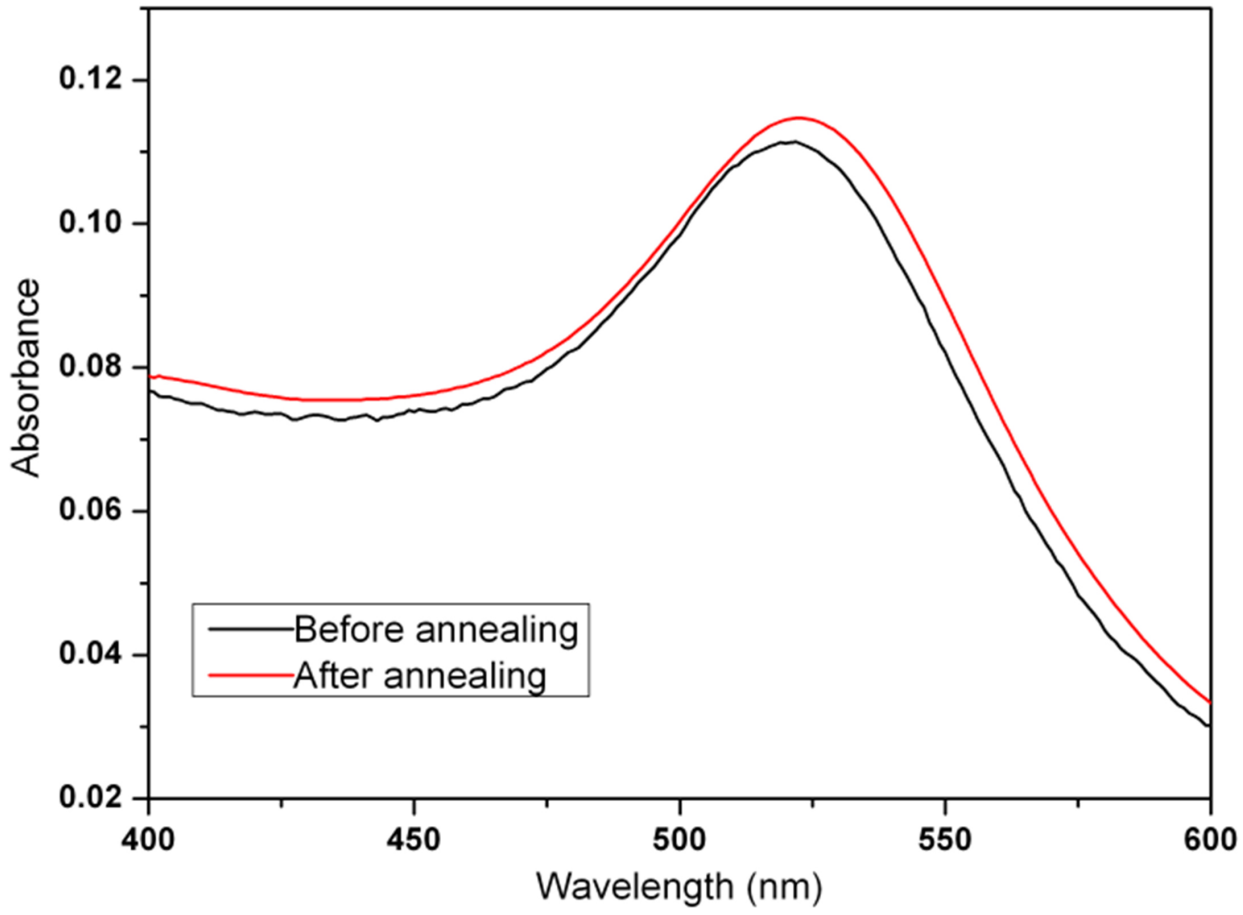

Fig. 7. UV-Vis absorption spectra of the mixture of DNA nanotube-AuNPs hybrid structures. UV-Vis, ultraviolet-visible.

with attachment sites were purified using Bio-rad purification columns, and 10 nm AuNPs were attached around them by probe hybridization, the hybrid structures were purified by agarose gel electrophoresis and the prepared DNA nanotubes-AuNPs heterostructures were characterized by TEM, and it was found that the AuNPs were in a helical arrangement around the DNA nanotubes and the number of AuNPs on each nanotube ranged from 7–9. The UV-Vis absorption spectra of the DNA nanotube-AuNPs revealed a red shift due to plasmonic resonance. This provides a foundation for the application of gold nanoparticles in optical sensing.

Several parameters strongly influenced the number of attached AuNPs per nanotube. The high DNA-to-AuNP functionalization ratio (1:300) aimed to ensure high surface coverage for stability and hybridization but may also introduce steric hindrance. The stepwise salt aging process (increasing NaCl to 300 mM) was crucial for screening electrostatic repulsion to facilitate hybridization. The 24-hour incubation with an excess of AuNPs (1:50 ratio) maximized attachment opportunity. However, electrostatic repulsion between closely spaced, negatively charged AuNPs likely became the limiting factor, preventing full occupancy of all 10 designed sites and leading to the observed heterogeneity.

While this study utilized established software and empirical optimization, integrating machine learning (ML) represents a powerful future direction. For instance, graph neural networks could be trained to predict the plasmonic coupling and chiroptical response of complex AuNP-DNA assemblies based on their spatial graph representation. Furthermore, reinforcement learning could optimize DNA origami templates—adjusting the number, spacing, and pattern of binding sites—to achieve target optical properties, moving beyond trial-and-error towards predictive design of plasmonic metamaterials [17,18].

Limitations

This study has several limitations. First, the attachment yield of AuNPs to the designed sites was heterogeneous, typically ranging from 7 to 9 per nanotube rather than the full 10. This is attributed primarily to increasing electrostatic repulsion as more AuNPs attach and potential steric hindrance from the high DNA density on the AuNP surface. Second, the observed plasmonic coupling, indicated by only a 4 nm red shift in UV-Vis spectra, was weak, suggesting suboptimal inter-particle coupling or a significant population of poorly coupled structures. Third, the assembly process relied on manual design and trial-and-

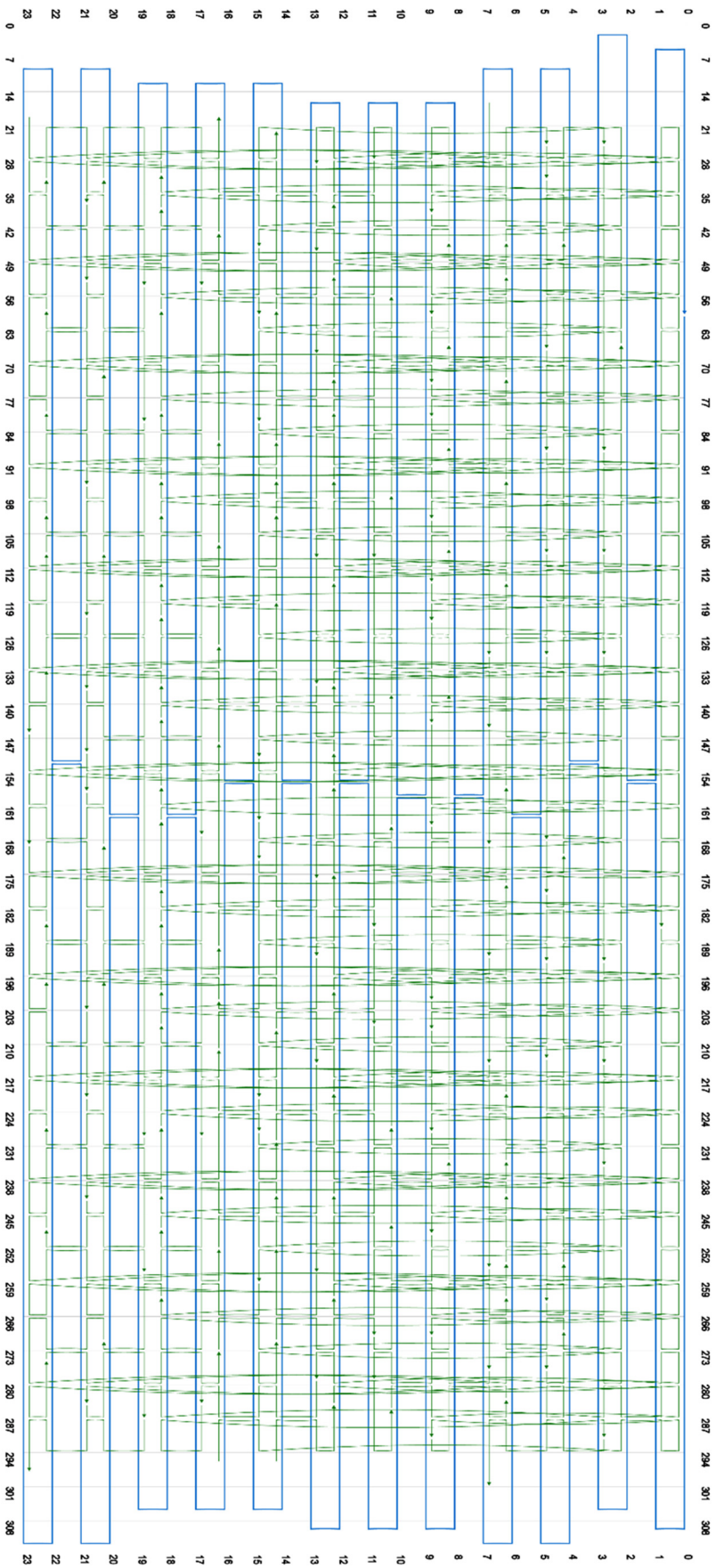

Fig. 8. Folding path diagram of DNA nanotube origami.

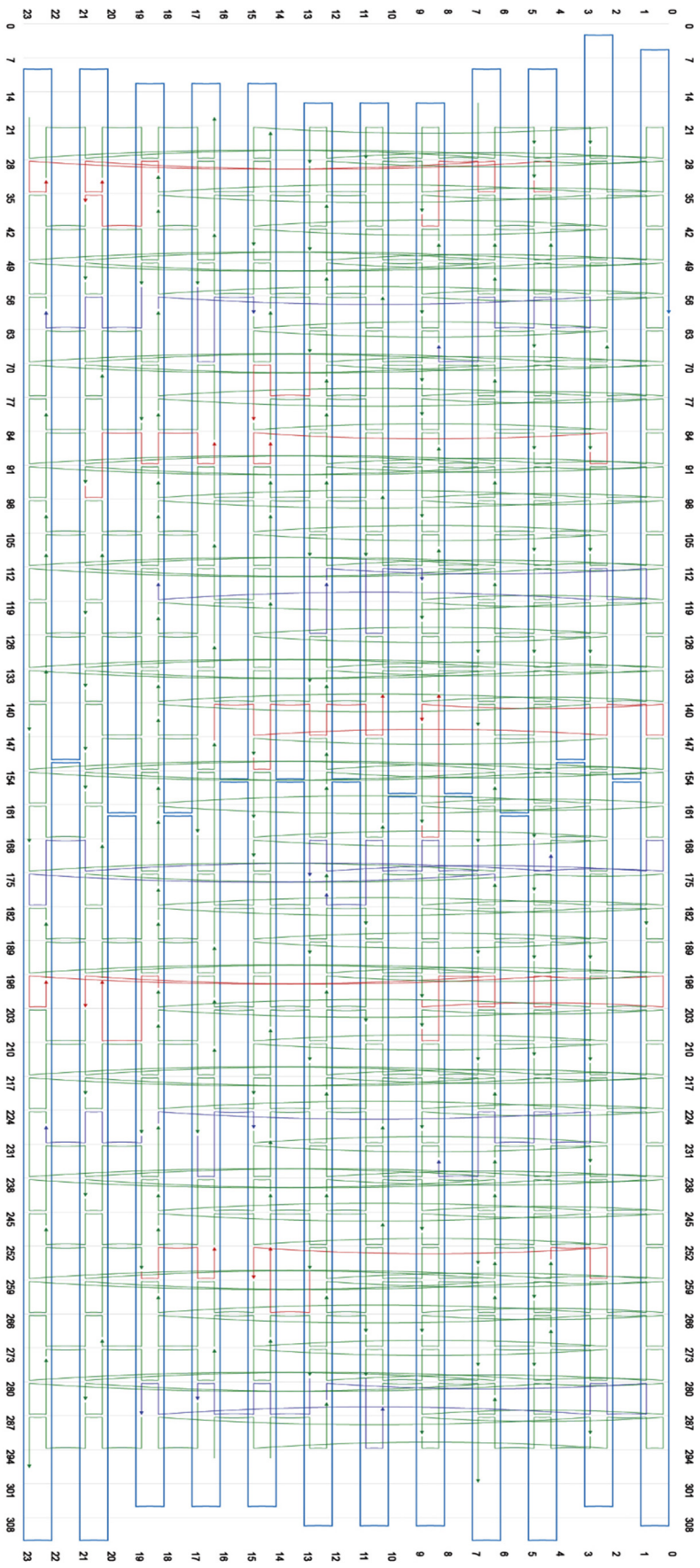

Fig. 9. Folding path diagram of DNA nanotube origami with connection sites.

Table 2. Staple sequence of DNA nanotube origami with connection sites and DNA probe sequence.

Number	Sequence	Length (nt)
A1	AATAATAATAATAATTTAAGCCAGGTTGATATAAGTATGGTTTAGCCGG	49
A2	AATAATAATAATAATAAAGATATGCAATTTAGATACGAACGACAAAGCGGATTGCAAAA	59
A3	AATAATAATAATAATTTTTAACCTCCGGCTTATTTAACAATTTCACGC	48
A4	AATAATAATAATAATGATTAGAGAGTACCTGCGGATGGC	39
A5	AATAATAATAATAATTTTCGCTACAAGGAGGCAGGAAAACTGA	43
A6	AATAATAATAATAATTTTATGCGTATGGTCGACACGACGTTAACCGAATACCGA	54
A7	AATAATAATAATAATTTGAGAATCGCCATATGCGAGAAAACT	42
A8	AATAATAATAATAATAAAATAGCAACTTTAAACACCATGTATCACCCC	48
A9	AATAATAATAATAATGAGCCTAATTTGCCAGTTGCGGGAGGTTTTAATC	49
A10	AATAATAATAATAATCCAACCTAATACTTAGCCGGAACCCCA	42
A11	AATAATAATAATAATAAGAAACTATCTTCTGAAAATACCTATCTTTATTAAATCCTTTGCTCAA	64
A12	AATAATAATAATAATTCAAAAGGGGAGTATCGTCGCGTCGCCCCAAATTCAACCGTTCTATTGC	64
A13	AATAATAATAATAATGATAGCCGATACCAGCACTTGAGATTA	42
A14	AATAATAATAATAATATTGTATGGACCACCCGATT	35
A15	AATAATAATAATAATTCATTATTGTTAAAATTCAAGTGTAGGT	43
B1	AATGGAACGGGAACGGGACGACAAAAAAAAAAAAAAA	37
B2	CTGGTTGGGTGAGCTCGTCAGTGAAAAAAAAAAAAAAAA	39
B3	ATAGGCACAGCATTAAATTCAAAAAAAAAAAAAA	35
B4	AACTAAAGAAATTGCGTAGACTTTATTAGAGCCGCCACAAAAAAAAAAAAAAAAAA	56
B5	CCAGCCTGAGTACCTGATTATCAGATGATGGCAAAAAAAAAAAAAAAA	48
B6	TTGATGGTGAACCAATAGCCAGCCACCCTCAAAAAAAAAAAAAAA	45
B7	ATAAGGATAAAAATTTTGAGACAGAAATATTTCTCTGACGGATAAAAAAAAAAAAAAA	59
B8	ATTCTTACCCAACATGCCTTATCATTCCAAAAAAAAAAAAAA	43
B9	TTACCAGACCCTTATGCGATTTTAAAAAAAAAAAAAA	38
B10	AATCATTTTCGAGCCAGATGTAATTCCAATCAACTATACAAGAAAACAAAAAAAAAAAAAAA	62
B11	CCCAATAGTTCATCGCTCGTTATGACGAGAGGGTTGCCTGAAAAAAAAAAAAAA	55
B12	GCAGAAGCCCTTTTTAAGGCGACAGGAAAAAAAAAAAAAA	41
B13	GAATCTCCAAAAAAAAGACTTTCAACAGTTAAAAAAAAAAAAAA	45
B14	AGGCAGGGAAAGAATAAATCCGCAAAAAAAAAAAAAA	38
B15	GTATATTTTGTCACAATCGAGGAAAATTGAGGCCATATCGTTTAAAAAAAAAAAAAA	58
C1	TTAAATCGGCCAAATGGCTCATATATTTTAATCAAAAGTAATA	43
C2	AGTTGTCTTTTTCAGCTAATG	21
C3	AATTCTGTCCCATCCTAGTCCTG	23
C4	AACCGATTAACCGCACTAGGTAAAGTAA	28
C5	AATAGCGGGAAAGCCGTAGAATATAAAGTAC	31
C6	GCGTCCACACCAAGAGTAACGAACTAACGGAATTCAACATAAATCTCAA	49
C7	CCAAAATTGTCCGGATAAAGAAAAATC	27
C8	TGCGTCATAGCAACGTATATACCAG	25
C9	AAAGGTCACGCGGATTCCGATGAAAGGCTATCAGGTCA	38
C10	AAGGAGTAGATGAGGCCAGAA	21
C11	AAAGCAACTGAAGCATACATA	21
C12	TCGTGTGAGCCTAGCATCTATTTTTGAG	28
C13	CGAGCTTGACGGGAAGAAAGAATATCATAATT	32
C14	GAACCGTCTAGTAGCGGATGGTTTTACAA	29
C15	ACACCAACGTACCACCATCATCTTAGCCAACGCTCAACTGTC	42
C16	TTACACTATTAATGCGCTCAAATACTTAA	29
C17	CCATTCCAGTTACTATGAAAGAACTTAACAACGC	34
C18	AAATCTGGTGTACCGCCTAGAAAGGAACAA	30
C19	TTTGTTCCGAATTGCGTAATGACCTAA	27
C20	TCAACGAAAATGCTTTCCTTAAACAAAAG	29
C21	AAATAACCGTGAACCCATTGTCGTCTTTCCATTTCG	36
C22	AACCCCTTCAGGCGGTTGACTGGAAAAACC	30

Table 2. Continued.

Number	Sequence	Length (nt)
C23	CAAAACATCGAAAGGGAGGCGCTAGTGATAATGTTT	36
C24	GCACCCTCAGTTTGCCATCTTTTCTATCACCGCGT	35
C25	TTAGAGCCGCGTCATAGCCCCCTTCCATTTGTAGAACCCGGCCTTGAGA	49
C26	GTTCCAGAGCGCGTTTTCATCGGCCAAAATCGGACATTGAAC	42
C27	TGGACAGGAGCCTTTAGCGT	20
C28	TCACAAACAAAATAGGTGTGCACCGTAATCAGGCCTT	37
C29	AGGTAAGCGTGGGGTTTTGCTCAGCCACCCTGAAGATCTACG	42
C30	AAATGGCCTTACGCTGGTCGTGCCATTGAATAAGAGCAACACTATGGCT	49
C31	AATGATGATAAAGAGAAGGATTAGTCATTTTCGACGACGATG	42
C32	GTATCATCAAGAGAGTTATCGGCCGCGGAATCTCGT	36
C33	ATCTAATAAGATTAAGAGGCTGAGCCAATAGGCAT	35
C34	AATGTGCCTTATTATTCTGAAA	22
C35	TTTAGAAGTATTAGATTTTGTCAGATATTAATTATCCTTG	40
C36	ACCTCAATATATTCATTTAATTACAGGTTGGGTTATATGCAA	42
C37	ATTATCATCATATTATAGCA	20
C38	GCCGTAGAACCTCAATAAAACAGTTGATTAAGAGGAAGCAAAC	43
C39	TCACAACGCATTTTCATTCTGGAAACTTCAAATATCGCAAAT	42
C40	GAGCATTATGCTAATAGCTGTAGCGACCGGAAGCAAACCAAT	42
C41	AGACTAAATCTCCAATAGCTTAATGGTCAG	30
C42	AAAAGTACCTTTCTGTAGCTTAGATTAAGACCGAC	35
C43	AATAACAATATATGTGAAGAGTCAATAGTGAAAAT	35
C44	GGTTTGCTTTGAAACAGAAAATCATAGGTCTGTTA	35
C45	TATAAAATCGTTTGAATTACCT	22
C46	ATTCAAGAAGGAAAATATCGACGATTGTAGCGA	33
C47	GGGGAAAAGGATATGCATTCGAGCTTCAAAGAATA	35
C48	AGATATTTGCACGTAAAAACTCGTAGGA	28
C49	ATTCGAAAAACCACCAGACAGAGAGGAATTAAAATT	36
C50	TGATAGAACCTACCATACCGAACGAAGG	28
C51	TACACTTCTGAATAATGAGTTTGAAACA	28
C52	AGAGAAGAGTCACACCGCTCACCAGAGCAAGGAAAGACACCA	42
C53	ATTAATCCTGATTGTTTTTGCGGATATC	28
C54	AGCAAAAGAAGATGAGTGAATAGCGAAAAATAAGCGCCCACC	42
C55	GCTAGAAGCCTTTATTTATATGATAAAC	28
C56	CTAACCCTGTAATACTTGCTGATATGAT	28
C57	ACAGGTTGTACCAAAAAAGGGTAGGTCA	28
C58	CAACTCAGAGCATAAAGTCTACAACGGT	28
C59	ACCTTGCTTTACATGAACCCTCCATTAACCTGAAAGTCA	39
C60	TTAATGGAATACCGTGGACTGAGGTGAATAAAAGACCA	38
C61	AAAATTCAATTAAGTGTTGCGCTGAGGGATTATAATG	37
C62	GATTTATGAAACAAACATTGTAAATGCTATAGTCAGAAGGTA	42
C63	AAGTACGGTGTTGGGGCCAGCAGGAAATAATGCCTCAGCAGA	42
C64	ATGTTTTAATGGCATCGCGGTCCCCTGTAGGAGGGGACAGG	41
C65	TTAGAAATCATACTGATTGAACCCGTTTGGTGTGAGT	37
C66	AAAACATGTTAAATAAGCGAAAAAAGAGAACATCAAAGA	39
C67	AAAGATTCCCAATTCTGCATTTCGAAAATCCTGTT	35
C68	AAAGGTTTCATTCCATATCCTGT	23
C69	ACATGCTGAATATAATGTAGTAGCGCCCTGACATT	35
C70	GCAGCGATAAATCGTCGCTATTAGAATATAATTTAGAACTG	41
C71	CGTGGGCGCTTAATCAGAGAACTCAATTGAGAAGCA	36
C72	TTATCACGCTGAATCCTGCTGGTAATCAGAGTACCAGAAGGAA	43
C73	CCTATTTATCTACATAAATCAATAACGG	28
C74	ATTCACCCGCTTAGACAATTACCGAGAG	28
C75	GACGTTGCTTGAATCAGACCTACACGCA	28

Table 2. Continued.

Number	Sequence	Length (nt)
C76	AAATTAGGCAGACATCAGTTGAGATACCCTGACTA	35
C77	TTGAATGGGGTGCCTAAATCAAAATTGA	28
C78	AATCGCTAACTGAGCCGGTTGGGAAGCTA	29
C79	GAGTGCGCTCTCACAATGGCCTCTATCG	28
C80	GCTAGTCGGGCTGTGTGGCTGGCGCCCTCAGAAGGAGCCTTTA	43
C81	TTCAGCTGCAAATCATGTGCAAGGGCCG	28
C82	ACTAACGCGCGGGTACCAACGCCAGAGG	28
C83	ACTAGATAGATAAATTTACGTTGCTATTACCAACGCTAACGCAAT	45
C84	AGTATCATAAACGCGCAATCAATGAAGCCTTTCCA	35
C85	CAACTAATAAGTTTTATTCAAGCAATCAAAAATGAAAATAGGG	43
C86	TACCACACAACATTGGCTGATTTGAAATCATGAGGAAGTTTAGCA	45
C87	TGCAGATACATTTAATAAAATCTTGAA	27
C88	GAATTACGAGCGTTGGGTTCA	21
C89	CAGTGCGTTAGAAATACGCTGAGAGTGAATA	31
C90	GACAATAAAAGTATAACTGA	20
C91	CAGTATTAAACGCGAGGTATTTATCCCAATCCAAA	35
C92	TTCAGTAGGGTATTTTAGAGAGACTACCTTTT	32
C93	CGACAAACATCGAGGCTTATCGAAACGATTTTTTGGAAT	39
C94	TACGAACGCCAGTTCAGACCG	21
C95	TCAGGAGCATAGTCCCCCTCGTTTTAAACTA	31
C96	CATACAAAGCTCCATGTAACGAAAGAGGCAAGTTA	35
C97	AAGAACTCATAACCCGTCATACGAACCATCAAC	33
C98	AATTAGACGATATAGCGTCTCCA	23
C99	TTTAATTTCGAGAGGCTAGTAAAATG	26
C100	ACCCTGTTTATCAACAAAAAAGCCATAAG	29
C101	GGCGTTTTTAGGCAAGTTCAATCGCGGG	28
C102	AATACGCCAGCGCGTACAAAGGGCGCC	27
C103	GGCGAAGTGTAAAGCCCGGCCATTCAATA	29
C104	GGCTATTACAGGTAGAAAGATTGGCAACAGACCA	34
C105	TTAGAGGCGCACTACGAAGGCA	22
C106	AATCTGTTTCAAACCTGTTTGCCCGCGA	28
C107	ATAAGGCGTGTCGACACTAAAACACTCAGGTCGCTGGGTTTTCGCA	46
C108	AAGATTAGAGCATGTACCGAGTAGGAGCGGCCCCCGCAGT	40
C109	TAGCGAACCTCCCGACTTACAAAATAAACACGCT	34
C110	TTCTAAGAACCAAGTAAGGGATTCGCGCTTAAAGAACAAGT	41
C111	ATATAGAAGAACAAGCGCTAAACGGGCGCGTTGGAACGCGA	41
C112	TGACCAACCCTTCATAACATACCACA	26
C113	GGGAAACGGGTAAAATACGAGAC	23
C114	TCAATCATACAAGAATATCCGCACTGCCCCCTGTTTAGCT	40
C115	GACCTGCTGCTCATAATTCGTTTAATGAGCAGCAAAATT	39
C116	ATAAATTTTGCCCTGATCCCCGGGGAGACCGCCTGATTA	39
C117	ACGGAGATTGAACGAGGCCTGCATGGGCGCGCAACAGCAGG	41
C118	AGACTTTTGAGGACAGATGAACGGTGTTTTTTACAGAGCTAA	42
C119	CAGCGATTATCCACGCATGTA	21
C120	AATCTTGCCTAATACGTGCCCTAACTAATAGACAAACAATTCGACACAG	49
C121	AATATATCCACTGGCCACAGAAGAATTGAGGTTATTAATTTTAAAGAAG	49
C122	GGTACGCAATAATAACGATAAGTTGCACCATCTGT	35
C123	GTCCCAGCCAACCAGTAGGCGGTCGCAAATCGTAACATTATCATTGGAT	49
C124	ACACAAAAGAACTGGCAGAAACGCCCG	27
C125	TAAACGCTCAGGCAGATCTGCAACCAATCAAACAAAGAAACC	42
C126	TTAGACTCCTTATTACGTAAAGGTCCATCGATAG	34
C127	AAGTTTTGACGCTCATCTGCTTTCTAGG	28

Table 2. Continued.

Number	Sequence	Length (nt)
C128	ACATTAGCAAACGAATTGCGAATAAGGCTTTGAGG	35
C129	AAGAGGCTGCCCAGGCACTGCATT	24
C130	CAGATAATTTTTTCACGGTGAGAAACCCTCACGAG	35
C131	ACGGGGCGATCACCGCTTCAGCTCTAAACGTGGTGAGAAAG	41
C132	AGCTCGCTATGCACTCCAGGAACGTATAAGCTCAAATCACCA	42
C133	CTTGTTTATCAGCTTGCGACGTTAAGCAAGCACTC	35
C134	AAGCGATTAACCAGTTTCCAGCTTCCCCGGTAATTAATGCCG	42
C135	CTTGTGAATTTCTTAAATA	19
C136	ACCAATAGAGAGCCAGATTT	20
C137	TAGTTGCCTCATAGGTCACCAGGAACCTGAGTAACAGTG	39
C138	AACCGATTGAGTCTTACCAGAAACATGAATCTTTTGCACCC	41
C139	CATATGGTTACAAAGTAGATAACCCAC	27
C140	CGGAGAATACCCCCTGAACAAATAACGGTA	30
C141	CTAAAGGTCTCAGGAAGCCCGGATAAATCC	30
C142	TCAGCGGATTGAAAACGAGGGTCCATTAACCGAAC	35
C143	AAGTTTGTACCGTGAAAGTTTTTAACGGGGTCACGTAAAAGAGT	44
C144	TGAATATAATCACCTCAGAACCGCCACTAA	30
C145	CCGGCCAAAGACAAAAGGAAAAGTTTAAGCCAGCGTCTTAAATC	44
C146	GAAAAAGTTTGGTTGAGGCAGGTCAAAACCCTAGTG	36
C147	AAAGGCAACATATAAAATGATTAAGACGGGATTTAACGATCAG	43
C148	CAATATATCGTCTGAAATAGCCAGCGAACCTCGCGGA	37
C149	GTAAGAAAATACATACACAGTATGTAAAAACAGCAGCCACCGCG	44
C150	AGAACCGTACCAGGATTTACCGTTCCAGAAGATTGCCA	38
C151	GCCGATTTTGCTAAACAGCTCCAACAGCGAATAATGCCAGACGG	44
C152	GATGTAAATGAATTTTCTGTATCGTTGCGGGATCG	35
C153	TTCTTAGCGTAACGATCCAGCTTGTATATTCTCTTTGATCGCCTG	45
C154	TCACCGGAACCAATTATTACAATATTAGT	29
C155	GCGAGCCACCACCCTCATCTAAAAGAAC	28
C156	TCGCACCAGAACCACCAGAAAGGATAAA	28
C157	AGCCGCCGCCAGCATTGTCAGTTGAGTA	28
C158	CAGATACCATTTCACACGTTGC	22
C159	CAGAATCCGTCACCTTACATTTGGA	25
C160	AGGAATGGAAAGCGCAGTAAATTGATTT	28
C161	AGTGCCGTGAACCGCTTTCCGGCGGT	26
C162	AGCCATACATGGCTTTTCAGA	21
C163	CTCCAGGAGTGTACTGGATAT	21
C164	CATAACACTAGATGGGCCCAGTCTCTAGAGGACGAGAATCATTGTG	46
C165	CCCTCAGAGCCGTCAATGCG	20
C166	GATATTCACCTTGCTAGCAAATCCGAGATCACGTATATGC	40
C167	AAATTTTCTTATAATGAGTGAAGGTCTTTTTAGGAA	36
Sa	ATTATTATTATTATTTTTT-SH	19
Sb	SH-TTTTTTTTTTTTTTT	16

error condition optimization. Finally, the potential chiroptical properties arising from the helical arrangement were not experimentally verified due to sample yield and purity constraints. Future work will focus on optimizing site design and assembly conditions to improve yield and coupling strength, and on integrating computational approaches like machine learning for inverse design.

5. Conclusions

In summary, double-layered DNA nanotubes with precisely positioned binding sites were successfully fabricated via DNA origami. Gold nanoparticles were conjugated to these sites, forming hybrid nanostructures with a helical arrangement of AuNPs around the nanotubes. Although the attachment efficiency and resultant plasmonic coupling require further optimization, this method demonstrates the potential of DNA origami as a programmable

template for creating complex plasmonic metamaterials. The integration of machine learning for design optimization presents a promising avenue for advancing this field towards tailored optical functionalities for sensing applications.

Availability of Data and Materials

The datasets used and analyzed during the current study are available from the corresponding author on reasonable request.

Author Contributions

XYang: Conceptualization, Data curation, Investigation, Writing-original draft. XYe: Conceptualization, Methodology, Funding acquisition, Writing-Review & Editing. MQ: Data curation, Investigation, Writing-Review & Editing. GW: Resources, Formal Analysis, Writing-Review & Editing. All authors contributed to editorial changes in the manuscript. All authors read and approved the final manuscript. All authors have participated sufficiently in the work and agreed to be accountable for all aspects of the work.

Ethics Approval and Consent to Participate

Not applicable.

Acknowledgment

Not applicable.

Funding

This work was supported by the National Natural Science Foundation of China [Grant No. 12272153], the Postgraduate Research & Practice Innovation Program of Jiangsu Province [Grant No. SJCX24_1797], and the Practice Innovation Program of Jiangsu University of Technology [Grant No. XSJCX23_18].

Conflicts of Interest

The authors declare no conflicts of interest.

Appendix

See Figs. 8,9, Table 2.

References

[1] Han L, Yu Y, Li P, Tian Y. From Nanoparticle Synthesis to Assembly: DNA as a Key Structural Material. RSC Applied Interfaces. 2026; 3: 26–44. https://doi.org/10.1039/D5LF00313J

[2] Mergny JL, Sen D. DNA Quadruple Helices in Nanotechnology. Chemical Reviews. 2019; 119: 6290–6325. https://doi.org/10.1021/acs.chemrev.8b00629

[3] Li K, Liu Y, Lou B, Tan Y, Chen L, Liu Z. DNA-Guided Metallization of Nanomaterials and Their Biomedical Applications. Molecules (Basel, Switzerland). 2023; 28: 3922. https://doi.org/10.3390/molecules28093922

[4] Kannappan S, Jo K, Kim KK, Lee JH. Utilizing peptide-anchored DNA templates for novel programmable nanoparticle assemblies in biological macromolecules: A review. International Journal of Biological Macromolecules. 2024; 256: 128427. https://doi.org/10.1016/j.ijbiomac.2023.128427

[5] Du L, Yang P, Xia L, Hu C, Yang F, Chen J, et al. Heteromultivalent DNA Enhances the Assembly Yield of Hybrid Nanoparticles and Facilitates Dynamic Disassembly for Bioanalysis Using ICP-MS. Analytical Chemistry. 2024; 96: 7194–7203. https://doi.org/10.1021/acs.analchem.4c00774

[6] Mendes BB, Conniot J, Avital A, Yao D, Jiang X, Zhou X, et al. Nanodelivery of nucleic acids. Nature Reviews. Methods Primers. 2022; 2: 24. https://doi.org/10.1038/s43586-022-00104-y

[7] Niu R, Du J, He W, Liu B, Chao J. DNA-Based Plasmonic Nanostructures with Tailored Optical Responses. Nano Research. 2025; 18: 94907197. https://doi.org/10.26599/NR.2025.94907197

[8] Liu M, Zhang X, Huang L, Li J, Fan C, Tian Y. DNA Nanostructure-Guided Plasmon Coupling Architectures. CCS Chemistry. 2023; 5: 568–588. https://doi.org/10.31635/ccschem.022.202202387

[9] Xie M, Hu Y, Yin J, Zhao Z, Chen J, Chao J. DNA Nanotechnology-Enabled Fabrication of Metal Nanomorphology. Research (Washington, D.C.). 2022; 2022: 9840131. https://doi.org/10.34133/2022/9840131

[10] Mucic RC, Storhoff JJ, Mirkin CA, Letsinger RL. DNA-Directed Synthesis of Binary Nanoparticle Network Materials. Journal of the American Chemical Society. 1998; 120: 12674–12675. https://doi.org/10.1021/ja982721s

[11] Li X, Wang J, Baptist A, Wu W, Heuer-Jungemann A, Zhang T. Crystalline Assemblies of DNA Nanostructures and Their Functional Properties. Angewandte Chemie (International Ed. in English). 2025; 64: e202416948. https://doi.org/10.1002/anie.202416948

[12] Zhan P, Peil A, Jiang Q, Wang D, Mousavi S, Xiong Q, et al. Recent Advances in DNA Origami-Engineered Nanomaterials and Applications. Chemical Reviews. 2023; 123: 3976–4050. https://doi.org/10.1021/acs.chemrev.3c00028

[13] Ding L, Liu B, Peil A, Fan S, Chao J, Liu N. DNA-Directed Assembly of Photonic Nanomaterials for Diagnostic and Therapeutic Applications. Advanced Materials (Deerfield Beach, Fla.). 2025; 37: e2500086. https://doi.org/10.1002/adma.202500086

[14] Douglas SM, Marblestone AH, Teerapittayanon S, Vazquez A, Church GM, Shih WM. Rapid prototyping of 3D DNA-origami shapes with caDNAno. Nucleic Acids Research. 2009; 37: 5001–5006. https://doi.org/10.1093/nar/gkp436

[15] Kuzyk A, Schreiber R, Fan Z, Pardatscher G, Roller EM, Högele A, et al. DNA-based self-assembly of chiral plasmonic nanostructures with tailored optical response. Nature. 2012; 483: 311–314. https://doi.org/10.1038/nature10889

[16] Storhoff JJ, Lazarides AA, Mucic RC, Mirkin CA, Letsinger RL, Schatz GC. What Controls the Optical Properties of DNA-Linked Gold Nanoparticle Assemblies? Journal of the American Chemical Society. 2000; 122: 4640–4650. https://doi.org/10.1021/ja9938251

[17] Wang H, Yang L, Leng D, Du Y, Ning H. Accelerating the discovery and optimization of metal-organic framework materials via machine learning. Advances in Colloid and Interface Science. 2025; 346: 103671. https://doi.org/10.1016/j.cis.2025.103671

[18] Yang H, Li H, Tang P, Lan X. Progress and perspective on chiral plasmonic nanostructures enabled by DNA programming methodology. Materials Advances. 2021; 2: 7336–7349. https://doi.org/10.1039/d1ma00781e